APPENDIX I

ANALYSIS OF SCOUR DATA AND MODIFIED RELIABILITY MODEL FOR SCOUR

1. INTRODUCTION

The AASHTO LRFD specifications (1998) state that "a majority of bridges that have failed in the United States and elsewhere have failed due to scour." This is confirmed by Shirole and Holt (1991), who observed that over the last 30 years, more than 1,000 of the 600,000 U.S. bridges have failed and that 60% of these failures are due to scour while earthquakes accounted for only 2%. Of course, there are many more bridges that are posted or otherwise taken out of service due to their inadequate strengths (e.g., due to deterioration, low rating, fatigue damage, etc.); nevertheless, scour is considered a critical cause of failure because its occurrence often leads to catastrophic collapses. For this reason, developing methods for the design and maintenance of bridge foundations subjected to risk from scour as well as developing tools to detect the presence of scour are currently considered top priorities for agencies concerned with the safety of bridges.

Scour is typically assessed using the methodologies presented in FHWA's Hydraulic Engineering Circular No. 18 (Richardson and Davis, 1995), known as "HEC-18." Although the HEC-18 model requires designing bridges to sustain foundation scour associated with the water flow depth and velocity corresponding to the 100-year or overtopping flood event, the remaining variables in the HEC-18 equations are considered to be deterministic. In other words, once the 100-year water depth and flow velocity have been estimated, the HEC-18 methodology, like most typical design procedures, uses a deterministic design approach with safety factors that implicitly account for uncertainties in the models, the parameters, or the hydraulic and hydrologic variables. The HEC-18 design equation for scour depth around bridge piers is given as follows:

$$\frac{y_{s\,\mathrm{design}}}{y_1} = 2.0 K_1 K_2 K_3 K_4 \left(\frac{D}{y_1}\right)^{0.65} F_0^{0.43} \tag{1}$$

where

$y_{s\text{ design}}$ = the nominal or design scour depth;
y_1 = the upstream flow depth;
D = the effective pier width;
F_0 = Froude number; and
K_1, K_2, K_3 and K_4 are correction factors for the pier shape, angle of attack, bed forms, and sediment gradation, respectively.

The flow depth, y_1, and the flow velocity used to calculate the Froude number are those corresponding to the 100-year or overtopping flood. The safety factors may be included in the bias factor of 2.0, the correction factors, K_i, and/or the usage of 100-year return period for y_1, which is longer than the 75-year design period stipulated for the design of bridges under the LRFD specifications.

If Equation 1 is developed to provide a safe (or nominal) value for scour depth, the actual depth of scour, $y_{s\text{ scour}}$, may be obtained from the following:

$$\frac{y_{s\,\mathrm{actual}}}{y_1} = 2.0 \lambda K_1 K_2 K_3 K_4 \left(\frac{D}{y_1}\right)^{0.65} F_0^{0.43} \tag{2}$$

where λ is a modeling factor which has an average value equal to 0.55 as reported by Johnson in Appendix B of this report.

If a bridge foundation is designed to satisfy Equation 1 and the actual depth of scour is obtained from Equation 2, the margin of safety, Z, can be defined as follows:

$$\mathrm{Z} = y_{s\text{ design}} - y_{s\text{ actual}}. \tag{3}$$

Failure would occur when $y_{s\text{ actual}}$ is greater or equal to $y_{s\text{ design}}$ or when the margin of safety, Z, is less than or equal to zero. Once the designer chooses the parameters of Equation 1 following the HEC-18 guidelines, $y_{s\text{ design}}$ will be exactly known. On the other hand, because of the randomness in the scour process, the determination of the actual scour depth $y_{s\text{ actual}}$ is associated with large uncertainties, and $y_{s\text{ actual}}$ must be considered to be a random variable. The sources of randomness are primarily due to the following.

- The modeling uncertainties associated with the HEC-18 equation, which does not provide very accurate estimates of scour depths even if all the input data are precisely known.
- The uncertainties associated with predicting the input data. These, as identified by Johnson (see Appendix B), are primarily due to the following:
  - The determination of the maximum 75-year discharge rate.
  - The determination of the flow depth and flow velocity corresponding to the 75-year discharge rate. Because for known channel profiles the flow and flow velocity are obtained from the discharge data based on Manning's roughness coefficient, the uncertainties are assumed to be primarily due to the determination of the appropriate Manning coefficient to use.
  - The random variation in river bed conditions and its influence on scour depth as represented by the factor K_3 in the above equations.

The prediction of the 75-year probability of failure, P_f, is defined as the probability that $Z \leq 0$ and can be estimated based on the statistical data describing the randomness of each of the variables that affect Equation 3, as described above and as listed in Table 1.

Although safety factors (or biases) may have been introduced into the empirically derived HEC-18 models, there is always a finite chance that the actual scour depth is larger than the design scour depth. This is due to the uncertainties associated with predicting the maximum flow depth and velocity that the river will be exposed to within the bridge's design period and the uncertainties associated with determining the correction factors, K_i, as well as the modeling errors that are introduced by the HEC-18 equations. The object of this appendix is to provide an explicit accounting for the uncertainties and the implied risks of the current scour design methodology in order to verify the compatibility between the safety of bridges subjected to scour and other loads and extreme events. To address issues related to structural risk, recent developments in bridge design procedures have used a reliability-based methodology to calibrate load and resistance safety factors. The goal of the calibration is to provide a consistent level of risk for the range of pertinent bridge geometries and loading conditions. The nominal measure of risk that is used during the calibration process is the reliability index, β, that is mathematically related to the probability of failure, P_f, by

$$\beta = \Phi^{-1}(P_f) \tag{4}$$

where Φ^{-1} is the inverse function of the cumulative normal distribution.

The reliability index, β, would give an exact measure of risk if all the random variables that affect the safety of the bridge component under consideration are properly identified along with their probability distribution types and pertinent statistics. Because of the difficulty of calculating P_f exactly, in most practical situations, the reliability index is calculated using approximate methods such as first or second order reliability method (FORM or SORM) algorithms or Monte Carlo simulations. Also, because many of the random variables that control the probability of failure are difficult to identify, categorize, and estimate and also because the statistical database for civil engineering applications is usually very limited, the reliability calculations would provide only a nominal measure of risk rather than an actuarial value. These limitations produce what is generally known as "modeling uncertainties."

To reduce the effects of the above-mentioned modeling uncertainties, the calibration of new design codes is often executed to match the reliability index obtained from existing "satisfactory" designs rather than satisfying a predetermined specific value for the probability of failure. This approach has worked reasonably well when calibrating load and resistance factors for bridges having typical geometries and materials having a long history of satisfactory performance under reasonably predictable loading conditions and when the reliability index, β, has been used as the primary criterion for developing new design codes. Analyses performed during the course of this study have demonstrated that the reliability index is highly controlled by the statistical properties of the modeling variable λ. For this reason, this appendix will focus on studying the modeling uncertainties associated with the scour design procedures and the influence of these uncertainties on the estimates of the reliability index. This analysis is based on the data provided by Landers and Mueller (1996) in their study supported by the FHWA.

2. SCOUR MODELING UNCERTAINTIES

For the reliability analysis of bridge piers subjected to scour, a Monte Carlo simulation can be used to generate random samples for each of the random variables that control the safety margin Z of Equation 3 based on their specified probability distributions. The estimation of the statistics including mean values and coefficients of variation (COVs) of the pertinent variables as well as the probability distribution types depend on each bridge's pier geometry, channel configuration, and channel bed properties. Evidently, several difficulties arise when attempting to estimate the properties of the

TABLE 1 Input data for reliability analysis for scour alone

Variable	Mean Value	Coefficient of Variation	Distribution Type	Reference
Q, discharge rate	From Table 2.8	From Table 2.8	Lognormal	Based on USGS website
λ_Q, modeling variable for Q	1.0	5%	Normal	Based on USGS website
λ_{sc}, modeling variable	0.55	52%	Normal	Johnson (1995)
n, Manning roughness	0.025	28%	Lognormal	Hydraulic Engineering Center (1986)
K_3, bed condition factor	1.1	5%	Normal	Johnson (1995)

variables that control scour at specific bridge sites, particularly when the bridge has not yet been constructed and actual measurements on the maximum scour depth are not available, even over limited periods of time. Even when such measurements may be available, the projection of the expected scour depth over the full design life of the bridge is associated with large levels of uncertainty. Added to these difficulties is the realization that the HEC-18 equations were primarily developed based on a limited number of small-scale laboratory experiments under "ideal" flow conditions and uniform sand bed materials that may not resemble actual field conditions. In fact, several investigations have shown large discrepancies between observed scour depths and those predicted from the HEC-18 equations. Because of all the limitations of the HEC-18 model, a procedure that takes into consideration the modeling uncertainties in an explicit manner while studying the safety of bridges subjected to scour is initiated in this appendix.

In assessing the safety of bridge piers subjected to scour, four broad sources of uncertainty are relevant: (1) inherent variability, (2) estimation error, (3) model imperfection, and (4) human error. Inherent variability, often called "randomness," may exist in the characteristic of the bridge structure or in the environment to which the structure is exposed. Inherent variability is intrinsic to nature and is beyond the control of the engineer or code writers. The uncertainties due to estimation error and model imperfection are extrinsic and, to some extent, reducible. For example, a reliability analyst may choose to obtain additional information to improve the accuracy of estimation. The uncertainty due to human error may also be reduced by implementing rigorous quality-control measures during the collection, interpretation, and analysis of scour data. Such improvements, however, usually entail an investment in time and money that the analyst may not be willing to undertake. In addition, this effort requires the capability of collecting such data at the site of interest. During the bridge design process when the bridge is still in the planning stages, the collection of site-specific data is not possible. Hence, it is usual to rely on design models developed based on data from other sites and for different bridge configurations and to project these available data to the particular site and bridge conditions. Hence, improving the quality of the data collection effort is not a viable option during the design stages, although this can be achieved at later stages when checking the safety of existing bridges. This study focuses on developing load factors for the design of new bridges under extreme events. Thus, the study must rely on available data collected from a variety of sites under different conditions to obtain estimates of the modeling uncertainties that describe the relationship between the expected scour depths and those predicted from the HEC-18 equations. In bridge engineering practice, pier scour depth is estimated using the HEC-18 model with Equation 1.

Field observations have shown that even when all the pertinent parameters of HEC-18 are known, large discrepancies still exist between the measured scour depths and those of the HEC-18 equations. These differences are attributed to the uncertainties in the HEC-18 model. To account for these modeling uncertainties, Equation1 can be modified by inserting a model correction factor, λ, which is defined as follows:

$$\lambda = \frac{y_{s\,\mathrm{actual}}}{y_{s\,\mathrm{design}}} \tag{5}$$

so that the actual depth of scour, $y_{s\ \mathrm{actual}}$, may be obtained from Equation 2. Notice that λ as defined in Equation 5 provides an inverse measure of safety such that a lower value of λ implies a higher level of safety. Also, since λ is a random variable, the higher its COV is, the higher the probability is that the actual depth of scour will exceed the design value and, hence, the lower the safety of the system is.

The mean value of λ is defined as $\bar{\lambda}$ and its standard deviation as σ_λ. These can be estimated from observations of scour depths at bridge piers and by comparing the observed scour depths with those predicted using the HEC-18 equation. For example, a 1996 study supported by FHWA has collected an extensive set of data on observed scour depths and compared these with different prediction models including the HEC-18 equations. The data published in the report by Landers and Mueller (1996) provides $y_{s\ \mathrm{actual}}$ and sufficient information to calculate $y_{s\ \mathrm{design}}$ for different sites, channel bed materials, and types of bridge piers. Table 2 provides a summary of the average values of λ and its COV for several different categories and groupings of the data.

A total number of 374 local scour measurements at different bridge piers were assembled from the report of Landers and Mueller (1996). Of these measurements, 240 were collected in channels with live-bed conditions and the rest were for piers set in clear-water conditions. Live-bed conditions occur when the water channel carries soil particles that are deposited on the channel floor at low flow speeds. These deposits would refill the scour hole such that under live-bed conditions, the scour process becomes cyclical. From Table 2, it is observed that the COV for the data collected in live-bed channels is lower than that obtained from all the data. Out of the 240 measurements taken in live-bed channels, 126 were for piers with rounded noses, 52 of the piers had square noses, 30 piers were cylindrical, and 32 had sharp noses. On the other hand, 191 of the bridges had single-pier bents and 49 had pier groups. The bridge piers were also classified based on three types of foundations: (1) piles, (2) poured, and (3) unknown. The soil type is classified as noncohesive soil or unknown soil. Only 18 data points satisfied the conditions of cylindrical single poured piers in live-bed channels having noncohesive soils. When all the data are analyzed simultaneously, the COV is 64.6%, indicating a very high level of modeling uncertainties. Large differences in the mean values

TABLE 2 Summary of mean and COV of λ based on data of Landers and Mueller (1996)

Flow and channel material type	Pier shape	Mean	Standard deviation	COV	Number of observations	Standard deviation of mean
All cases		0.412	0.266	0.646	374	0.0138
Channels with live-bed conditions only		0.429	0.247	0.576	240	0.0159
All channel bed material	Rounded	0.400	0.231	0.577	126	0.0206
	Sharp	0.523	0.292	0.558	32	0.0516
	Cylinder	0.383	0.204	0.532	30	0.0372
	Square	0.432	0.246	0.570	52	0.0341
Noncohesive soils	All shapes	0.417	0.237	0.569	195	0.0170
Unknown soil type	All shapes	0.479	0.283	0.593	45	0.0422
Single piers	All shapes	0.405	0.223	0.550	191	0.0161
Pier groups	All shapes	0.535	0.310	0.580	49	0.0443
Pile foundation	All shapes	0.421	0.256	0.607	158	0.0204
Poured foundation	All shapes	0.419	0.185	0.442	67	0.0226
Unknown foundation	All shapes	0.547	0.361	0.660	15	0.0932
Noncohesive soils, poured	Rounded	0.405	0.181	0.446	48	0.0261
Noncohesive soils, poured	Cylinder	0.355	0.132	0.371	18	0.0311

and/or COVs are observed for different pier shapes, foundation types, and so forth. Lower COVs are observed when the data are categorized based on pier shape and streambed conditions. As an example, the mean value of λ for the 18 cases that have cylindrical poured piers in noncohesive soils was found to be 0.36 with a COV of 37.1%. The piers with rounded noses produced a mean value of λ equal to 0.41 with a COV equal to 44.6%. The lowest value of COV is observed for the case of cylindrical piers in poured foundations set in live-bed channels with noncohesive soils. Presumably, this lower COV of 37.1% reflects the fact that the HEC-18 model was primarily developed based on laboratory simulations under these same conditions. Although the lowest in Table 2, a COV of 37.1% still indicates a high spread in the observed data away from the mean value. The bias of 0.36 for this case implies a conservative design equation with an implicit safety factor on the order of 2.82 (1/0.36).

The point estimates of the mean and the standard deviations of λ given in Table 2 are obtained from a limited set of data. To convey information on the degree of accuracy of these estimates, one should recognize that λ is a random variable with (unknown) mean μ_λ and with (unknown) standard deviation σ_λ. The sample means that values of $\bar{\lambda}$ given in Table 2 are estimates of μ_λ for various data sets. The precision of these estimates can be assessed using the fact that a sample mean $\bar{\lambda}$ is a random variable with mean value equal to μ_λ and a standard deviation of $\sigma_{\bar{\lambda}} = \sqrt{(\sigma_\lambda)^2/n}$ where n is the sample size. It is noted that for large sample sizes, $\bar{\lambda}$ will approach a normal distribution, and the confidence intervals for $\bar{\lambda}$ may be obtained using the normal probability tables. The data of Landers and Mueller (1996) also provide estimates of σ_λ (column 4 standard deviation) from which $\sigma_{\bar{\lambda}}$ is calculated as given in the last column of Table 2. Notice how, in many instances, as the classification of the data is narrowed to specific categories of pier shapes and water channel conditions, the standard deviation (σ_λ) decreases; however, since the number of samples used to calculate $\bar{\lambda}$ decreases also, the standard deviation of $\bar{\lambda}$ (i.e., $\sigma_{\bar{\lambda}}$) increases, thus expressing a lower level of precision in the estimation of $\bar{\lambda}$.

The data from all 374 cases are plotted in a histogram, as is shown in Figure 1. The figure also shows the histograms that would be obtained if the data were assumed to follow a normal distribution or a lognormal distribution. The plots seem to indicate that the modeling variable λ may be reasonably well modeled by a lognormal distribution. Further verification of this observation for different subsets of the data is undertaken below.

The data from the live-bed channels consisting of 240 data points are also plotted using a lognormal probability scale, as is shown in Figure 2. The plot further verifies that λ for this set of data may be reasonably well represented by a lognormal distribution. Other probability plots for different sets of data are provided in Figures 3, 4, and 5. In particular, Figure 3 plots the modeling factor λ for rounded poured piers set in live-bed channels with noncohesive soils on a normal probability curve. Figure 4 plots the same data on a lognormal probability scale. Figure 5 gives a plot on a lognormal scale for the data assembled for cylindrical poured piers in live bed-channels with noncohesive soils. It is noted that Figures 3 and 4 show that the distribution of λ for the rounded piers approaches a normal distribution near the upper part of the curve (i.e., for high values of λ) while for low values of λ, the probability distribution more closely approaches that of a lognormal distribution. On the other hand, a lognormal distribution seems to be appropriate for the cylindrical piers, as shown in Figure 5.

The chi-squared goodness-of-fit tests for the data sets plotted in Figures 2 through 5 were executed as summarized in Tables 3 through 6. The results confirm the observations made

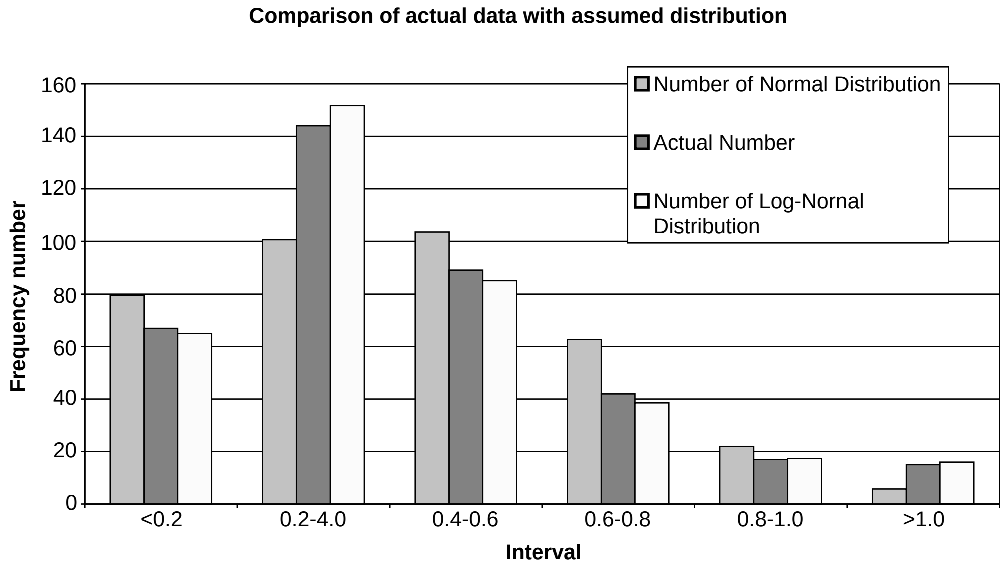

Figure 1. Histogram for distribution of λ.

from the probability plots. In particular, the chi-squared test for the complete data as depicted in Table 3 shows that the data are not inconsistent with the assumption that the underlying distribution is lognormal with a significance level of 5%. In fact, the sum of the squared difference between the observed frequencies and the corresponding lognormal frequencies divided by the lognormal frequency produced a sum equal to 1.02, which is lower than the value of the appropriate χ_f^2 distribution at the cumulative probability of 95%, which is given in probability tables as $C_{1-\alpha,\,f} = 7.81$ where $\alpha = 5\%$ and $f = 3$. On the other hand, the assumption of a normal distribution produces a sum of the squared difference equal to 45.86, which is much higher than $C_{1-\alpha,\,f} = 7.81$. Table 4 shows the same results for the data set consisting of 240 samples collected at sites with live-bed conditions. Table 5 gives the results for the scour-modeling ratio, λ, for the 48 rounded poured piers set in noncohesive soils in live-bed channels. Table 6 gives the same analysis for the cylindrical piers. It is noted that for all the cases considered, the lognormal distribution is acceptable within the 5% confidence level. However, Table 5 shows that for the rounded piers, the normal distribution would also be valid.

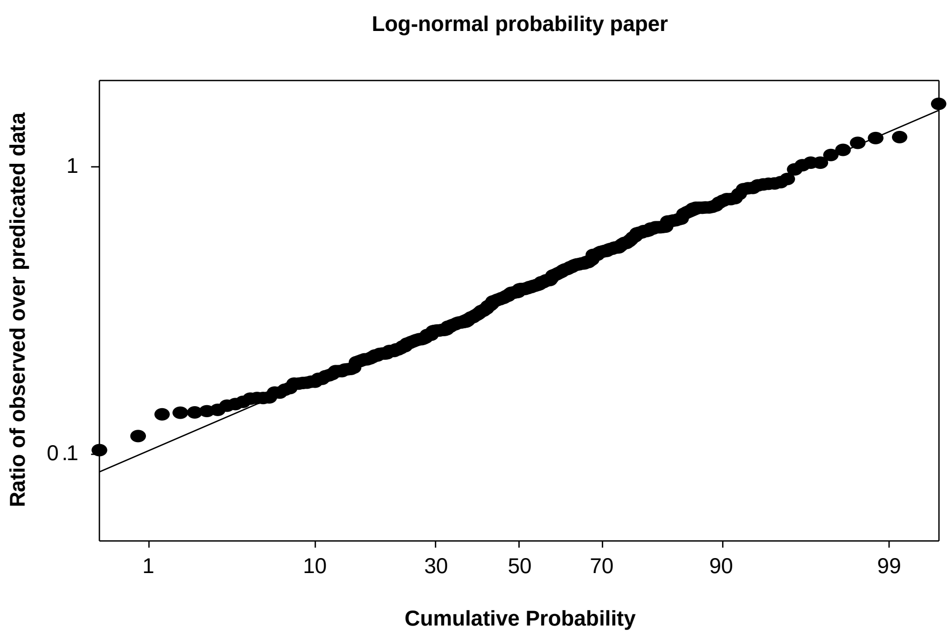

Figure 2. Plot of data from live-bed conditions on lognormal probability paper.

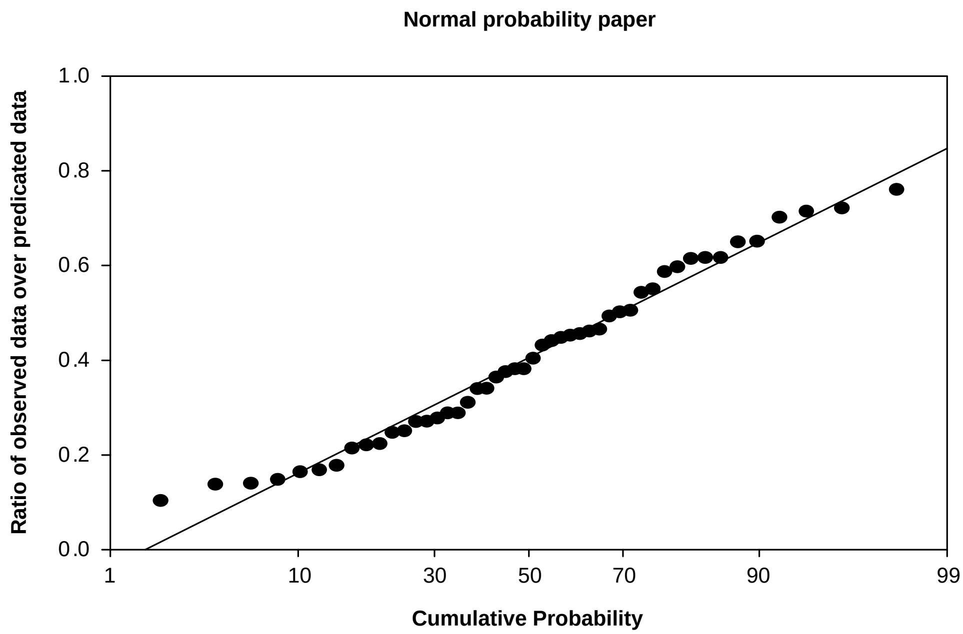

Figure 3. Plot of data for rounded piers under live bed on normal probability paper.

Currently used reliability analysis procedures account for modeling uncertainties by including λ in the failure function and treating it as a random variable in a similar way as all the other physical variables that affect the safety of a structural system. However, the use of a single modeling variable λ for all scour cases assumes that the expected ratio between the observed scour and the scour predicted from the HEC-18 equations is constant for all levels of scour and is independent of any of the parameters that control scour at a given site. This is not necessarily the case. A plot of λ versus the logarithm of the observed scour depth is shown in Figure 6. The plot shows how the modeling variable varies with the observed scour depth for the 48 samples corresponding to scour in noncohesive soil around rounded poured piers. The

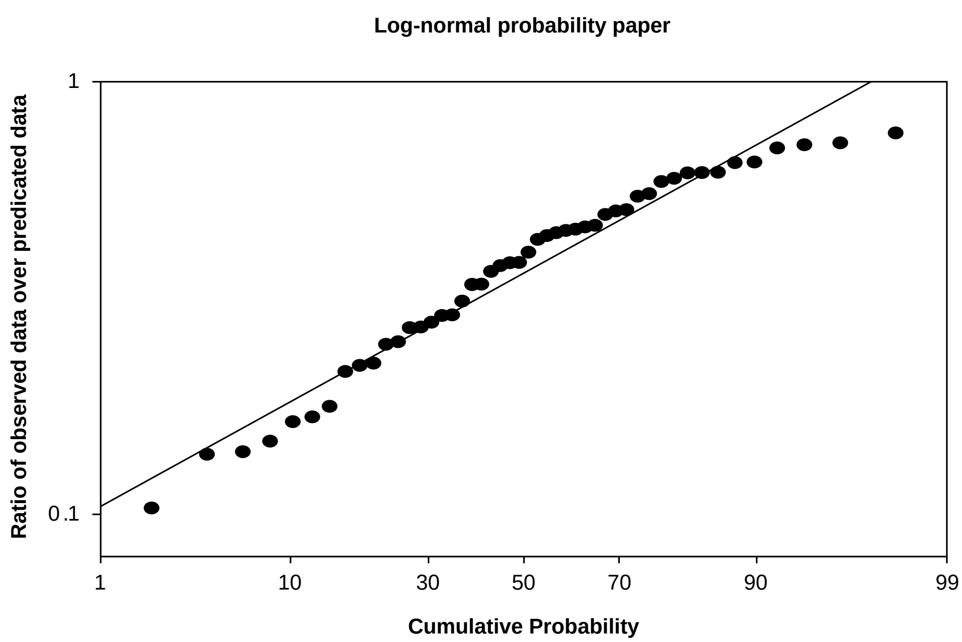

Figure 4. Plot of data from rounded piers under live bed on lognormal probability paper.

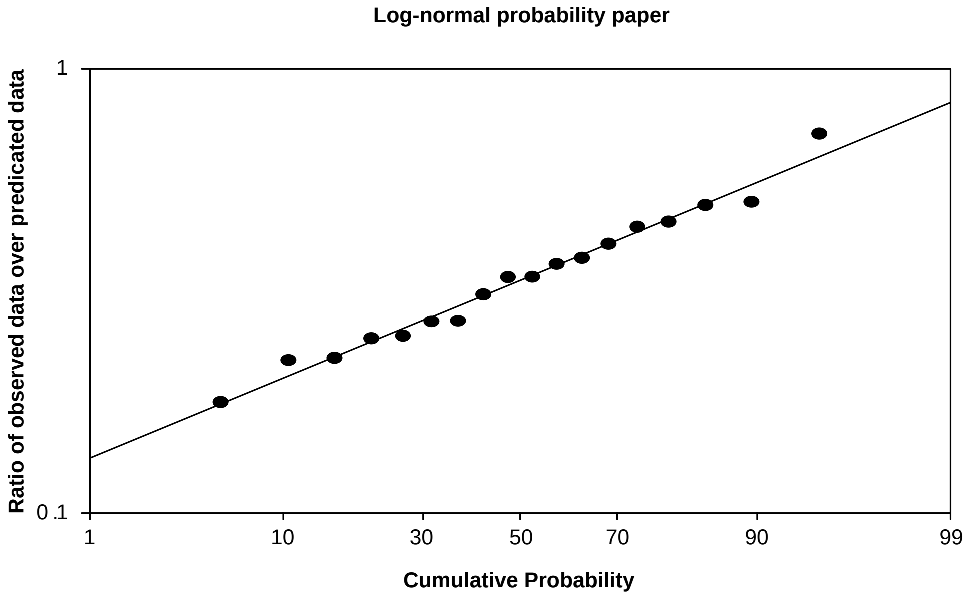

Figure 5. Plot of data for cylindrical piers under live-bed conditions on lognormal probability paper.

TABLE 3 Chi-squared goodness-of-fit test for λ using all scour data

Frequency Range	N_i Observed	e_i, Normal Distribution	e_i, Lognormal Distribution	$(N_i-e_i)^2/e_i$ for Normal	$(N_i-e_i)^2/e_i$ for Lognormal
< 0.2	67	79.5	65	1.97	0.06
0.2–0.4	144	100.6	151.7	18.72	0.39
0.4–0.6	89	103.5	85.1	2.03	0.18
0.6–0.8	42	62.7	38.5	6.83	0.32
0.8–1.0	17	22	17.3	1.14	0.01
> 1.0	15	5.7	16	15.17	0.06
Sum	*374*			*45.86*	*1.02*
$C_{1-\alpha,f}$				*7.81*	*7.81*

TABLE 4 Chi-squared goodness-of-fit test for λ using scour data from live-bed channels

Frequency Range	N_i Observed	e_i, Normal Distribution	e_i, Lognormal Distribution	$(N_i-e_i)^2/e_i$ for Normal	$(N_i-e_i)^2/e_i$ for Lognormal
< 0.2	36	30.7	29.8	0.91	1.29
0.2–0.4	100	86.5	109.2	2.10	0.77
0.4–0.6	55	89.1	62.5	13.02	0.89
0.6–0.8	29	30.3	24.1	0.05	0.98
0.8–1.0	11	3.35	8.8	17.50	0.53
> 1.0	9	0.12	5.6	660.64	2.06
Sum	*240*			*694.22*	*6.51*
$C_{1-\alpha,f}$				*7.81*	*7.81*

plot of Figure 6 clearly shows skewness in λ. Other plots and a regression analysis indicate that λ increases asymptotically as the observed scour depth increases. The relationship between λ and the scour depth may be represented by an equation of the following form:

$$\lambda = 0.24 y_s^{0.49}. \tag{6}$$

The standard error for the above equation is found to be $\varepsilon = 0.464$ and the multiple $R^2 = 0.42$. Alternatively, a multivariable regression analysis of λ as a function of the pier width, D, flow depth, y_1, and flow velocity, V, shows that λ can be represented in an equation of the form

$$\lambda = 0.184 + 0.0081 D + 0.0044 y_1 + 0.014 V. \tag{7}$$

TABLE 5 Chi-squared goodness-of-fit test for λ using scour data of rounded piers in live-bed channels

Frequency Range	N_i Observed	e_i, Normal Distribution	e_i, Lognormal Distribution	$(N_i-e_i)^2/e_i$ for Normal	$(N_i-e_i)^2/e_i$ for Lognormal
< 0.2	7	6.14	5.96	0.12	0.18
0.2–0.3	10	7.30	11.25	1.00	0.14
0.3–0.4	7	10.00	10.59	0.90	1.21
0.4–0.5	9	10.16	7.60	0.13	0.26
0.5–0.6	6	7.65	4.89	0.36	0.25
0.6–0.7	5	4.28	3.01	0.12	1.32
> 0.7	4	2.47	4.71	0.95	0.11
Sum	*48*			*3.58*	*3.47*
$C_{1-\alpha,f}$				*9.49*	*9.49*

TABLE 6 Chi-squared goodness-of-fit test for λ using scour data of cylindrical piers in live-bed channels

Frequency Range	N_i Observed	e_i, Normal Distribution	e_i, Lognormal Distribution	$(N_i-e_i)^2/e_i$ for Normal	$(N_i-e_i)^2/e_i$ for Lognormal
< 0.2	1	2.15	1.31	0.62	0.07
0.2–0.3	6	3.93	5.52	1.09	0.04
0.3–0.4	5	5.31	5.66	0.02	0.08
0.4–0.5	4	4.16	3.22	0.01	0.19
0.5–0.6	1	1.88	1.41	0.41	0.12
0.6–0.7	0	0.49	0.55	0.49	0.55
> 0.7	1	0.08	0.33	10.54	1.36
Sum	*18*			*13.18*	*2.42*
$C_{1-\alpha,f}$				*9.49*	*9.49*

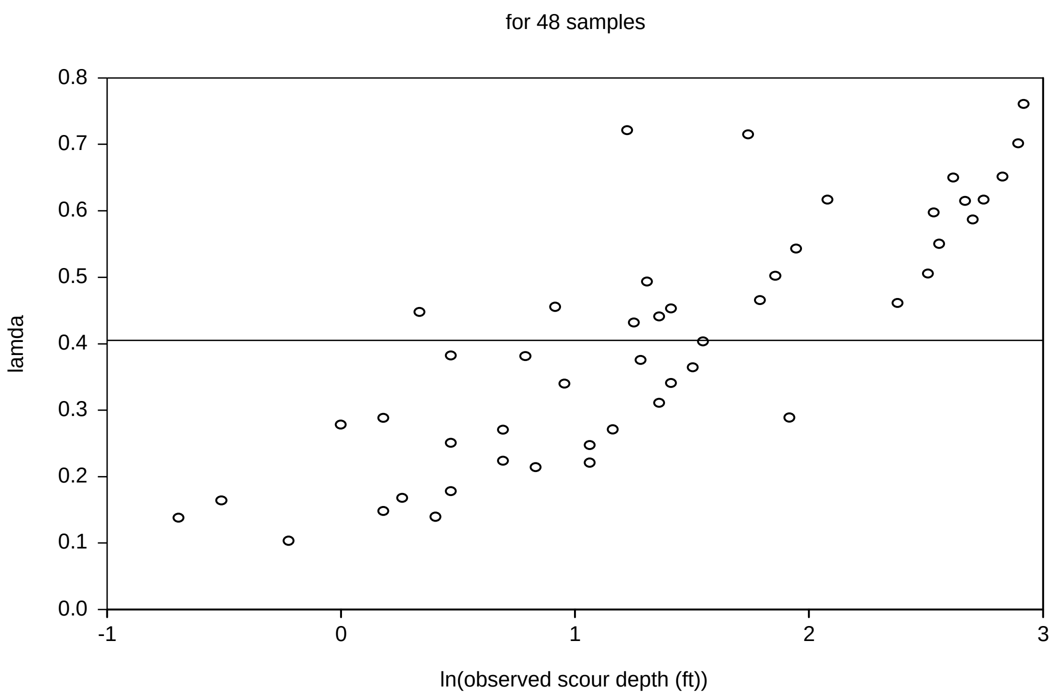

Figure 6. Plot of modeling variable, λ, versus observed scour depth.

The above equation is executed for the 48 samples of rounded piers in noncohesive soils under live-load conditions. In fact, using an analysis of variance, it was found that the effect of the pier shape on the average value of λ was not statistically significant given the high observed standard deviations.

To account for the skewness in λ that is caused by the use of the HEC-18 equations, an alternative method of analysis is suggested as described in Section 3 of this appendix.

3. ALTERNATIVE RELIABILITY MODEL FOR SCOUR

Appendix C of this report presented the results of a reliability analysis of bridge piers subjected to scour. The model used in Appendix C was based on data that were previously available in the literature and assumed that the modeling variable λ is uniform for all cases. The existence of the extensive database published by Landers and Mueller (1996) provides a unique opportunity to come up with an alternative empirical model for predicting scour depths based on a multivariable regression analysis. Several alternative regression models have been analyzed, including a regression effected on the whole data set consisting of 374 samples, on the 48 samples for the rounded piles in noncohesive soils, and on the combination of rounded and cylindrical piers.

Based on the parameters tabulated by Landers and Mueller (1996) and after several trials to identify the parameters that control the scour depth, the regression equation for the total 374 sample size was selected to be of the following form:

$$\begin{aligned}\ln(\text{scour}) \sim\ & \text{shape} + \text{bed-load transport} \\ & + \ln(\text{pier width}) + \ln(\text{flow depth}) \\ & + \ln(\text{flow velocity})\end{aligned} \tag{8}$$

where ln is the log function. The regression coefficients obtained using the S+ computer package are tabulated as shown in Table 7; the residual standard error was found to be 0.56, and the term $R^2 = 0.53$.

The regression analysis of the 48 samples of rounded piers in noncohesive soils was performed using a model of the following form:

$$\begin{aligned}\ln.(\text{scour}) \sim\ & \ln(\text{pier width}) + \ln(\text{flow depth}) \\ & + \ln(\text{flow velocity})\end{aligned} \tag{9}$$

In this case, the regression coefficients are listed in Table 8. The residual standard error was found to be 0.41 on 44 degrees of freedom and the term R^2 is 0.83.

The analysis of the residuals for the 48 sample points as plotted in Figures 7 through 9 shows that the points are evenly spread around the value of 0.0 and that they can be reasonably well represented by a normal distribution.

The use of the regression results in the reliability analysis may be effected by replacing the failure function of Equation 3 by the equation

$$Z = y_{\text{design}} - y_{\text{regression}} \tag{10}$$

where for rounded piers in noncohesive soils $y_{\text{regression}}$ is calculated from

$$\begin{aligned}\ln y_{\text{regression}} =\ & -2.08 + 0.63 \ln D + 0.48 \ln y_1 \\ & + 0.61 \ln V + \varepsilon\end{aligned} \tag{11}$$

where

D = the pier diameter,
y_1 = the flow depth,
V = the flow velocity, and
ε = the residual error.

TABLE 7 Coefficients of regression analysis for all 374 samples of data

Coefficients				
	Value	**Standard Error**	***t* Value**	***Pr* (> |*t*|)**
(Intercept)	–0.60	0.10	–6.10	0.000
Shape 1	–0.19	0.11	–1.68	0.094
Shape 2	–0.10	0.04	–2.47	0.014
Shape 3	–0.02	0.03	–0.67	0.500
Shape 4	0.02	0.02	0.96	0.338
Bed.load	0.16	0.03	4.60	0.000
ln.width.b	0.66	0.07	9.58	0.000
ln.flow.depth	0.20	0.04	5.04	0.000
ln.flow.vel	0.12	0.05	2.15	0.032

TABLE 8 Coefficients of regression analysis for 48 samples of rounded pier data

Coefficients				
	Value	**Standard Error**	***t* Value**	***Pr* (> |*t*|)**
(Intercept)	–2.08	0.30	–6.98	0.0000
ln.width.b	0.63	0.14	4.62	0.0000
ln.flow.depth	0.48	0.13	4.10	0.0002
ln.flow.vel	0.61	0.13	4.78	0.0000

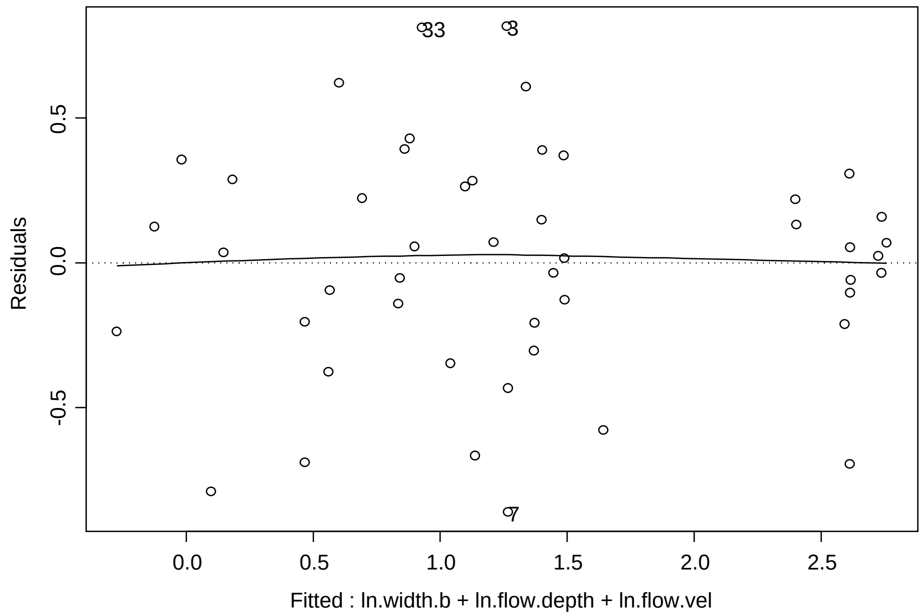

Figure 7. Plot of residuals for 48 samples of rounded piers.

As explained above, D is a deterministic variable since the pier diameter can be accurately known even before the actual construction of the pier; y_1 and V are random variables that depend on Manning's roughness coefficient and the 75-year maximum discharge rate, which are random variables having the properties listed in Table 8. Based on the analysis of the residuals effected in this section of the report, ε may be considered to follow a normal distribution with mean equal to zero and a standard deviation equal to 0.41.

Using Equation 10 in a Monte Carlo simulation as described in Section 2 of Appendix C of this report for the Schohaire River, data would lead to the results shown in Figure 10. The plot shows that if the HEC-18 equation is used for designing the bridge pier, then the critical design scour depth should be $y = 17.3$ ft. The reliability index obtained for such a design is $\beta = 0.47$. The reliability index increases to $\beta = 2.71$ when the scour depth is designed to be twice the value of HEC-18 (i.e., $y_{actual}/y_{HEC\text{-}18} = 2.0$ or $y_{actual} = 34.6$ ft).

A slight difference in the results is observed when $y_{regression}$ is calculated based on the regression equation obtained when the full set of 374 samples is used (i.e., from Equation 8). These results are also shown in Figure 10. In this case, the

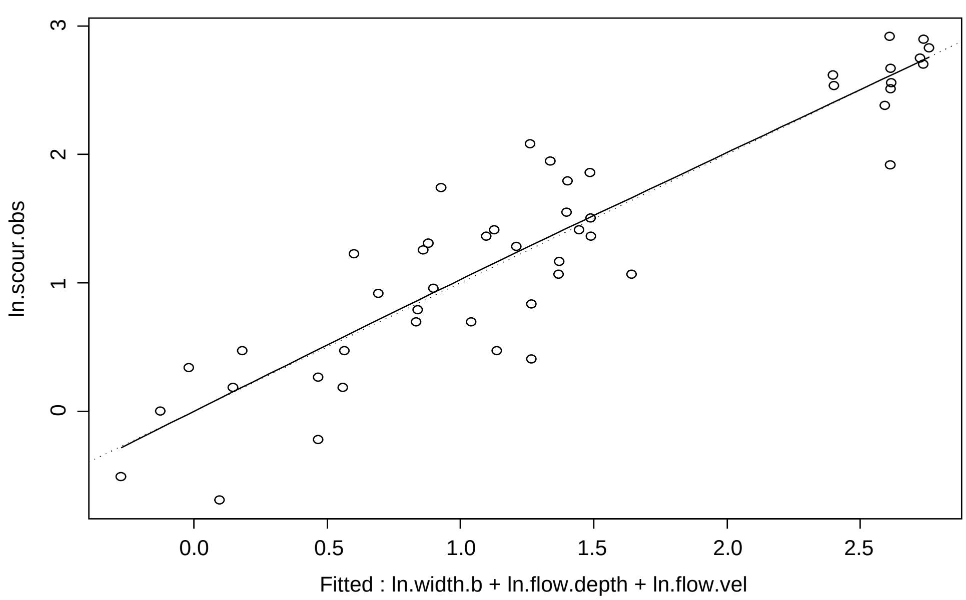

Figure 8. Comparison of regression results to observed scour depth.

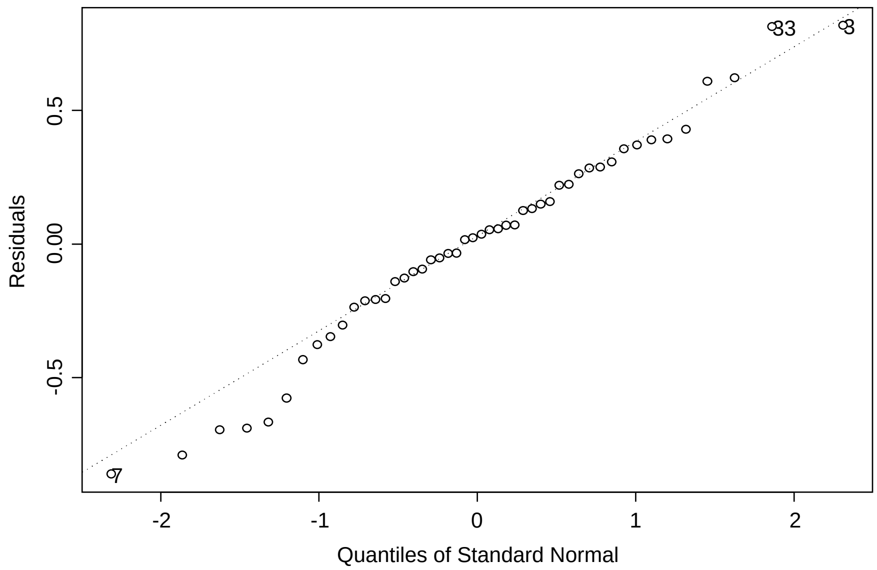

Figure 9. *Plot of residual versus standard normal quantiles.*

reliability index of β = 0.58 is obtained when the foundation is designed for a critical depth of 17.32 ft as stipulated from the HEC-18 equations. The reliability index is 2.45 when the foundation depth is set at 34.64 ft. The small differences observed between the results obtained from Equation 8 and Equation 9 are due to the larger standard regression error obtained from Equation 8 that uses all 378 sample points.

The reliability analysis is subsequently performed for the five different rivers that were analyzed in Appendix C: the Schohaire, Mohawk, Sandusky, Cuyahoga, and Rocky Rivers. These relatively small rivers are selected because they produce 100-year flood depths ranging from 8.5 ft to 21 ft, which are appropriate for the bridge configuration under investigation as described in Appendix C. As was done in Appendix C, two cases are considered: (1) the case in which the bents are formed by one column each and (2) the case in which the bents are formed by two columns. The results of the reliability analysis for each case are presented in Figures 11 and 12.

Tables 9 and 10 also provide a summary of the results obtained using this alternative reliability model for the bridge with the one-column bent and for the two-column bent. The results illustrate how the reliability index decreases for the

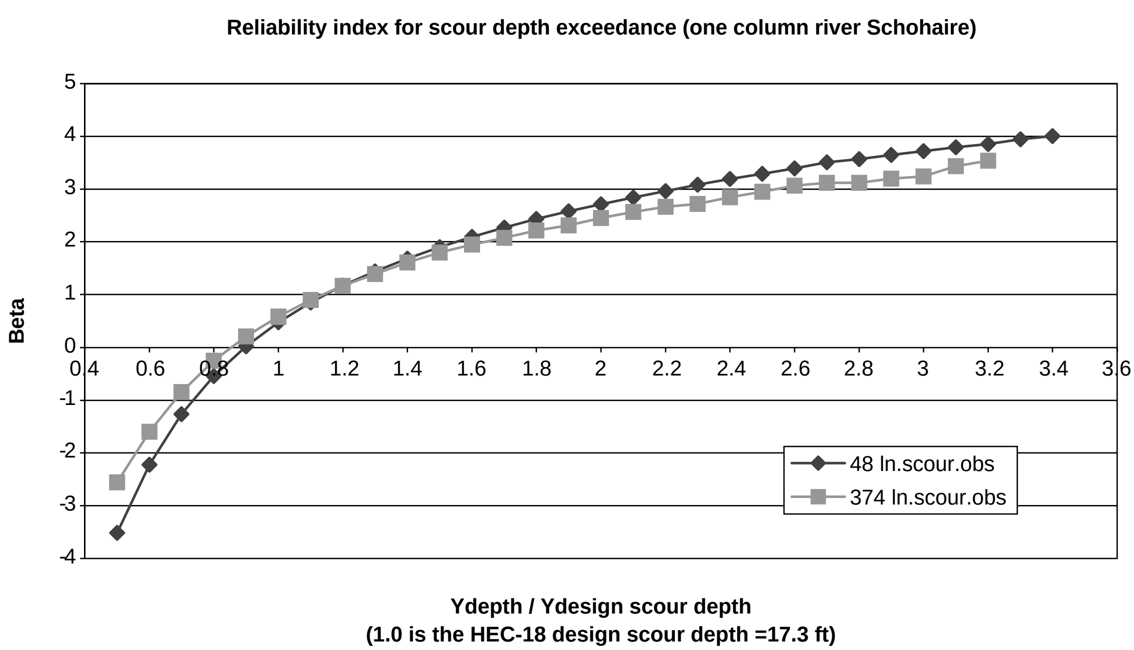

Figure 10. *Plot of reliability index versus foundation depth.*

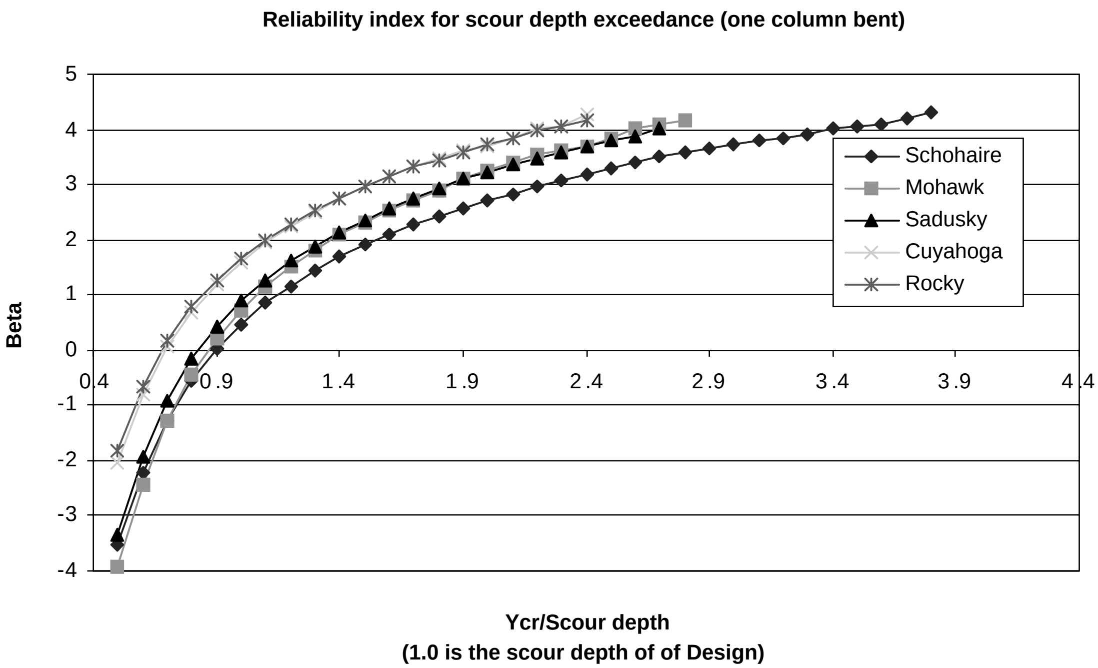

Figure 11. Plot of reliability index for one-column bent for five river discharges.

rivers with higher discharge rates varying from $\beta = 1.66$ for the Rocky River to $\beta = 0.47$ for the Schohaire River. The lower beta for the rivers with higher discharge rates reflects the influence of a lower modeling variable, λ, for high values of scour depths. Such results indicate that the HEC-18 equation becomes less conservative as the expected scour depth increases. The average reliability index for the cases considered is on the order of 1.08. If one is to group the rivers into three categories—high discharge rates (Schohaire), medium discharge rates (Mohawk and Sandusky), and small discharge rates (Cuyahoga and Rocky)—then the average beta would be close to $\beta = 1.0$. This value is clearly lower than the $\beta = 1.40$ observed in Appendix C when the reliability model employing a uniform modeling variable is used.

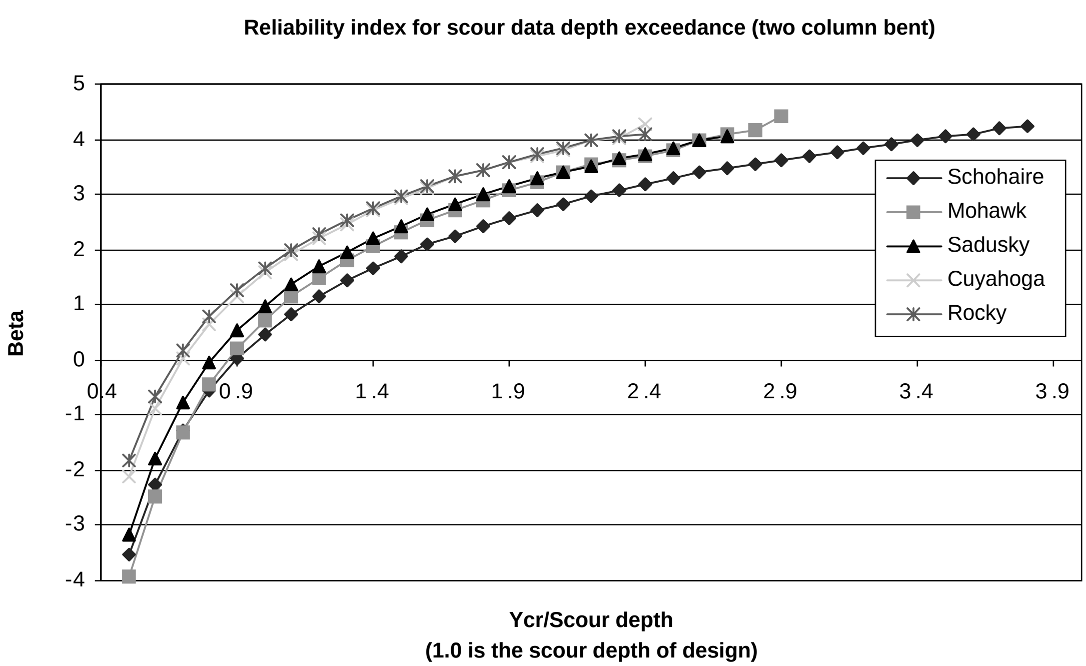

Figure 12. Plot of reliability index for two-column bent for five river discharges.

TABLE 9 Summary of reliability analysis for one-column bent for different river discharge data

River	Average *Ys*75 (max scour depth in 75 yr)	COV of *Ys*75	Design depth (ft)	Reliability index, β
Schohaire	16.29	25%	17.3	0.48
Mohawk	12.56	21%	14.0	0.73
Sandusky	12.03	22%	14.3	0.90
Cuyahoga	8.88	21%	12.3	1.60
Rocky	8.68	22%	12.3	1.66

TABLE 10 Summary of reliability analysis for two-column bent for different river discharge data

River	Average *Ys*75 (max scour depth in 75 yr)	COV of *Ys*75	Design depth (ft)	Reliability index, β
Schohaire	11.60	25%	12.3	0.47
Mohawk	8.95	21%	9.9	0.71
Sandusky	8.57	22%	10.2	0.99
Cuyahoga	6.33	21%	8.7	1.57
Rocky	6.18	22%	8.75	1.65

4. CONCLUSIONS

This appendix presented an analysis of the scour data published by Landers and Mueller (1996). A new reliability model was then proposed based on the results of the analysis. The reliability calculations have shown that the HEC-18 model provides varying levels of reliability depending on the expected scour intensity at a site. In particular, the use of HEC-18 for designing the foundations of bridge piers provides higher safety levels for rivers with relatively small discharge rates (differences in the reliability index on the order of 1.20 are observed for the sites selected in this appendix). In all cases, however, the reliability index observed for bridge foundations designed according to the HEC-18 equations are much lower (on the order of $\beta = 1.0$) than those of bridge members designed for gravity loads using the current AASHTO LRFD specifications, which produce a reliability index on the order of 3.5. Adding a load safety factor on the HEC-18 equations will help increase the average reliability index as observed in Section 3.2 of the main body of this report. However, a major review of the HEC-18 equations will be needed in order to reduce the spread in the observed reliability levels between different sites.

The model proposed herein is based on a regression fit for the data of Landers and Mueller (1996), which is limited to sites with observed scour depths less than 20 ft. The model may not be appropriate for use for sites at which the scour depth is expected to exceed this value.

REFERENCES FOR APPENDIX I

American Association of State Highway and Transportation Officials (1998). *AASHTO LRFD Bridge Design Specifications,* 2nd edition, Washington, DC.

Hydraulic Engineering Center (1986). “Accuracy of Computed Water Surface Profiles,” U.S. Army Corps of Engineers, Davis, CA.

Johnson, P.A. (1995). “Comparison of Pier Scour Equations Using Field Data,” *ASCE Journal of Hydraulic Engineering,* Vol. 121, No. 8; pp. 626–629.

Landers, M.N., and Mueller, D.S. (1996). “Channel Scour at Bridges in the United States,” FHWA-RD-95-l84, Federal Highway Administration, Turner-Fairbank Highway Research Center, McLean, VA.

Richardson, E.V., and Davis, S.R. (1995). *Evaluating Scour at Bridges*, 3rd edition. Report No. FHWA-IP-90-017, Hydraulic Engineering Circular No. 18, Federal Highway Administration, Washington, DC.

Shirole, A.M., and Holt, R.C. (1991). “Planning for a Comprehensive Bridge Safety Assurance Program,” *Transportation Research Record 1290*, Transportation Research Board of the National Academies, Washington, DC; pp. 39–50.